ACS APPLIED MATERIALS & INTERFACES

Research Article

www.acsami.org

Thermo-Sensitive Polymer-Grafted Carbon Nanotubes with Temperature-Controlled Phase Transfer Behavior between Water and a Hydrophobic Ionic Liquid

Yue Wang,[†,‡] Wenguang Leng,[†] Yanan Gao,*[,†] and Jiansheng Guo*[,‡]

[†]Dalian Institute of Chemical Physics, Chinese Academy of Sciences, 457 Zhongshan Road, Dalian 116023, P. R. China

[‡]College of Textiles, Donghua University, Shanghai 201620, P. R. China

ABSTRACT: Thermo-sensitive polymer-grafted carbon nanotubes were prepared by surface-initiated atom transfer radical polymerization and carefully characterized. A reversible, temperature-induced phase transfer behavior of these organic−inorganic hybrids between water (with a decrease in temperature to 20 °C) and a hydrophobic ionic liquid, 1-ethyl-3-methylimidazolium bis(trifluoromethylsulfonyl)imide ([Emim]NTf_2) (with an increase in temperature to 90 °C), was observed. Mechanism analysis suggests that this reversible phase transfer between water and [Emim]NTf_2 is due to the relative affinity of the two solvents for the poly(ethylene oxide) units grafted on the carbon nanotubes. Our results pave the way for further design of carbon nanotube-based, recyclable phase transfer vehicles as well as heterogeneous catalysts suited for a water−hydrophobic ionic liquid biphasic system.

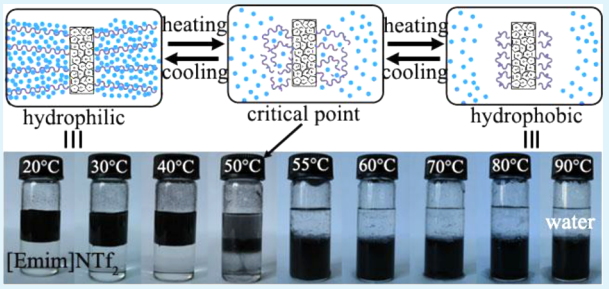

KEYWORDS: *thermo-sensitive, atom transfer radical polymerization, carbon nanotube, phase transfer, ionic liquid*

1. INTRODUCTION

The efficient transfer of substances, such as molecules, supramolecular assemblies, nanoparticles, etc., across the interface of two immiscible liquid phases (typically an oil−water interface or a hydrophobic ionic liquid−water interface) is of great significance for applications such as phase transfer catalysis, separation, and targeted drug delivery.[1−5] It would be more interesting if such behavior could be induced by outside stimuli to produce intelligent, reversible, and quantitative cargo transportation. Preliminary attempts in this area have produced appealing outcomes.[6,7] For instance, Desset et al. prepared a novel catalyst that could be triggered to move back and forth between water and toluene by bubbling with and removal of CO_2.[6] Similarly, Horton et al. succeeded in preparing a series of "hairy" silica nanoparticles via surface-initiated atom transfer radical polymerization (ATRP), which can be reversibly transported between water and a hydrophobic ionic liquid through temperature regulation.[7]

Carbon nanotubes (CNTs) are ideal carriers for loading inorganic nanoparticles as heterogeneous catalysts[8−10] because of their tubular morphology, mechanical strength, and chemical stability.[11,12] However, CNTs are prone to form intertwined aggregations with poor dispersity in solvents, which restricts their further processing. To overcome this drawback, covalent grafting of polymers onto the surface of CNTs has been proposed. For instance, the surface-initiated ATRP approach has been successfully used to control the thickness of the polymer layer decorated at the surface of CNTs.[13,14] Even so, CNTs as phase transfer shuttles for delivering substances between immiscible liquids are still rarely reported. The limited paradigm includes the following. Marcilla et al. found that polymer-decorated CNTs can be used as vehicles for repeated transfer of nano-objects between aqueous and organic phases.[15] Unfortunately, laborious and time-consuming anion exchange treatments for achieving the desired effect are unavoidable, making the strategy less automatic.

Room-temperature ionic liquids (RTILs) are a series of tunable solvents with many unique physicochemical properties, including negligible vapor pressure, favorable thermal stability, wide liquid temperature ranges and electrochemical windows, etc.[16] Because of their attractive properties, RTILs have been widely used as alternative media for chemical reactions and extraction or separation.[17] Therefore, it is of interest to find more carriers that can be transferred reversibly between two environmentally friendly solvents, that is, a hydrophobic ionic liquid and water.

In this work, multiwalled CNTs (MWCNTs) grafted with a thermo-responsive polymer were fabricated via surface-initiated ATRP. Interestingly, the obtained composites showed an obvious, quick, and reversible phase transfer behavior between water and a common hydrophobic ionic liquid, 1-ethyl-3-methylimidazolium bis(trifluoromethylsulfonyl)imide ([Emim]NTf_2), under temperature control. This smart nanodevice can work spontaneously and continuously without

Received: December 16, 2013
Accepted: March 3, 2014
Published: March 3, 2014

   dx.doi.org/10.1021/am405796c | *ACS Appl. Mater. Interfaces* 2014, 6, 4143−4148

Scheme 1. General Procedures for the Synthesis of MWCNTs-Poly(PEGMMA)

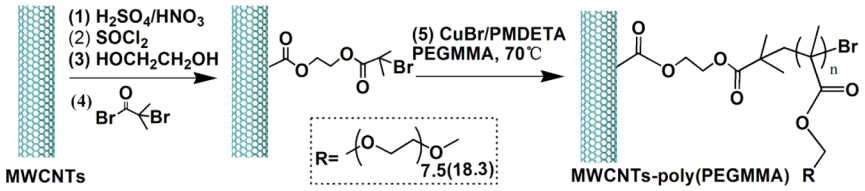

excess post-treatment steps. To confirm the effectiveness of this approach, two macromonomers [poly(ethylene glycol) methyl ether methacrylate with an average relative molecular weight of 475 (PEGMMA-475) or 950 (PEGMMA-950)] were both subjected to ATRP, producing thermo-sensitive MWCNTs-poly(PEGMMA-475) and MWCNTs-poly(PEGMMA-950). The results of this work pave the way for the further design of a CNT-based, recyclable phase transfer catalyst suited for a water−hydrophobic ionic liquid biphasic system.[18]

2. EXPERIMENTAL SECTION

2.1. Materials. MWCNTs (purity of >95 wt %, length of 10−30 μm, outer diameter of 10−20 nm, inner diameter of 5−10 nm) were provided by Chengdu Organic Chemical Co. 2-Bromoisobutyryl bromide (98 wt %), 4-dimethylaminopyridine (DMAP, 99 wt %), triethylamine (TEA, 99 wt %), *N*,*N*,*N*′,*N*″,*N*″-pentamethyldiethylenetriamine (PMDETA, 99 wt %), PEGMMA-475, and PEGMMA-950 were purchased from Aladdin-reagent Co. and used without further purification. CuBr (99.999 wt %) was purchased from Sigma-Aldrich.

2.2. General Procedures for the Synthesis of MWCNTs-Poly(PEGMMA). Following a literature procedure[19] with some changes, five steps are included as shown in Scheme 1. (1) MWCNTs were ultrasonicated and cut in a H_2SO_4/HNO_3 mixture before carboxyl groups were introduced onto their surfaces, generating MWCNTs-COOH. (2) Thionyl chloride reacted with a carboxyl group to produce MWCNTs-COCl. (3) Hydroxyl groups were introduced by reaction of MWCNTs-COCl with ethylene glycol to yield MWCNTs-OH. (4) Initiating sites for ATRP were formed by reacting MWCNTs-OH with 2-bromoisobutyryl bromide, producing MWCNTs-Br. (5) Grafting polymerization of PEGMMA-475 (with 7.5 units of ethylene oxide) and PEGMMA-950 (with 18.3 units of ethylene oxide) macromonomers onto MWCNTs-Br was conducted by surface-initiated ATRP, resulting in MWCNTs-poly(PEGMMA-475) and MWCNTs-poly(PEGMMA-950) as the final products.

2.2.1. Synthesis of MWCNTs-COOH. In a typical experiment, raw MWCNTs (4.0 g) were suspended in a mixture of concentrated H_2SO_4 (98 wt %) and HNO_3 (70 wt %) (160 mL, volume ratio of 3:1) and then ultrasonicated for 10 h. The resultant suspension was rinsed with a large amount of water until the mixture became neutral. The filtered solid was dried under vacuum at 75 °C, giving MWCNTs-COOH (3.4 g).

2.2.2. Synthesis of MWCNTs-COCl. MWCNTs-COOH (1.0 g) was dispersed in $SOCl_2$ (80 mL) and stirred at 75 °C for 24 h. The solid was separated and dried under vacuum at ambient temperature for 2 h, yielding MWCNTs-COCl (0.85 g).

2.2.3. Synthesis of MWCNTs-OH. The as-prepared MWCNTs-COCl (0.7 g) was mixed with ethylene glycol (80 mL) and stirred at 120 °C for 48 h. The solid was washed with anhydrous tetrahydrofuran (THF) and dried in vacuum at 70 °C overnight.

2.2.4. Synthesis of MWCNTs-Br. All operations were conducted under a nitrogen atmosphere. MWCNTs-OH (0.30 g) was placed in anhydrous $CHCl_3$ (20.0 mL) before DMAP (0.02 g) and TEA (0.23 g) were added. Then, 2-bromoisobutyryl bromide (0.50 g) dissolved in anhydrous $CHCl_3$ (5 mL) was added dropwise at 0 °C within 60 min. The mixture was further stirred at 0 °C for 3 h, followed by stirring at room temperature for an additional 48 h. The filtered solid was washed with $CHCl_3$ and dried under vacuum at 40 °C for 8 h, affording MWCNTs-Br (0.3 g).

2.2.5. Synthesis of MWCNTs-Poly(PEGMMA-475). MWCNTs-Br was the only ATRP initiator used in our experiment; no other free radical initiators were ever added. Typically, MWCNTs-Br (0.4 g), CuBr (0.29 g, 2.0 mmol), PMDETA (0.35 g, 2.0 mmol), and *N*,*N*-dimethylformamide (DMF) (25 mL) were placed in a dried flask sealed with a rubber plug. The flask was air-evacuated and backfilled with N_2 three times before PEGMMA-475 (5.0 g) was added. The ATRP reaction proceeded at 70 °C for 24 h. After several washing (with $CHCl_3$, THF, and water) and centrifugation cycles, MWCNTs-poly(PEGMMA-475) can be successfully separated from impurities and dissociative homogeneous linear polymers formed during polymerization.

2.2.6. Synthesis of MWCNTs-Poly(PEGMMA-950). All the manipulations are similar to those of MWCNTs-poly(PEGMMA-475), except for reactant dosage: MWCNTs-Br (0.35 g), CuBr (0.14 g, 1.0 mmol), PMDETA (0.17 g, 1.0 mmol), and PEGMMA-950 (5.0 g).

2.3. Characterization. The morphology of MWCNTs-poly(PEGMMA) was observed by transmission electron microscopy (TEM) (Tecnai G2 F30, FEI Co.) at 300 kV. Fourier-transform infrared (FTIR) measurements were taken on a Bruker spectrophotometer (model TENSOR27) in the range of 4000−400 cm^{-1} with powder-pressed KBr pellets. Thermal stability was measured via thermogravimetric analysis (TGA) (STA449F3, NETZSCH) in the range of 40−850 °C at a heating rate of 10 °C/min (N_2 flow rate of 20 mL/min). Raman spectra were recorded on a Raman spectrometer (Bruker, SENTERRA) using 532 nm laser excitation. Water contact angles (WCAs) were measured using an optical contact angle measuring device (KRUSS, DSA100). ^1H nuclear magnetic resonance (NMR) spectra were recorded on a Bruker Avance III 400 MHz NMR spectrometer using D_2O as a solvent.

3. RESULTS AND DISCUSSION

3.1. Morphology and Structures of MWCNTs-Poly(PEGMMA). The morphology of resultant samples was observed using TEM as shown in Figure 1. Panels a and b of Figure 1 display the images of MWCNTs-poly(PEGMMA-475). The darker MWCNT shell was wrapped by a brighter polymer layer, and the coverage thickness was in the range of 2−4 nm. A more obvious polymer layer in the range of 4−8 nm was demonstrated for MWCNTs-poly(PEGMMA-950) instead, as shown in panels c and d of Figure 1. This difference in polymer layer thickness is largely caused by the variation in the molecular weight of composed macromonomers. PEGMMA-950 contains approximately 18.3 ethylene oxide units, more than double the amount for PEGMMA-475 (only 7.5 ethylene oxide units). In other words, the thickness of the polymer grafted onto MWCNTs can be tuned by varying the molecular weight of constructed moieties.

The structure of the intermediates obtained from each synthetic step was analyzed by FTIR spectra as shown in Figure 2. The characteristic absorption at 1638 cm^{-1} for the C═C vibration,[19] the strong band at 1724 cm^{-1} due to the C═O stretching vibration,[20] and the 1571 cm^{-1} peak for the MWCNT skeletal in-plane vibration[21] can be observed for all the intermediates (Figure 2a−d). After ATRP, the greatly intensified bands at 2871 cm^{-1} (attributed to the C−H stretching vibration)[22] and the newly emerging signal at 1104

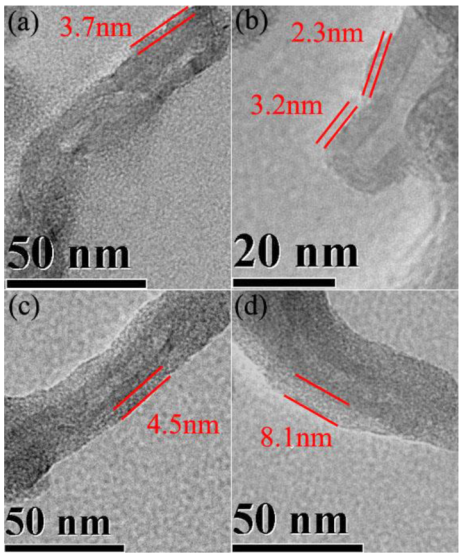

Figure 1. TEM images of (a and b) MWCNTs-poly(PEGMMA-475) and (c and d) MWCNTs-poly(PEGMMA-950).

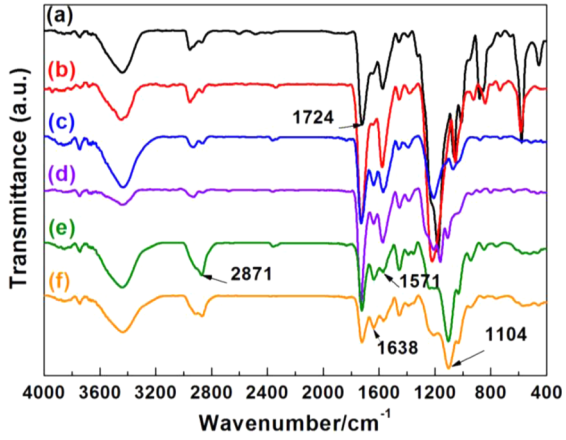

Figure 2. FTIR spectra of (a) MWCNTs-COOH, (b) MWCNTs-COCl, (c) MWCNTs-OH, (d) MWCNTs-Br, (e) MWCNTs-poly(PEGMMA-475), and (f) MWCNTs-poly(PEGMMA-950).

cm^{-1} (assigned to the C−O stretching vibration)[23] in spectra e and f of Figure 2 suggest the successful grafting of poly(PEGMMA) onto MWCNTs, consistent with the observed TEM images.

The weight loss curves of MWCNTs-COOH, MWCNTs-OH, MWCNTs-Br, MWCNTs-poly(PEGMMA-475), and MWCNTs-poly(PEGMMA-950) were all investigated by TGA as shown in Figure 3. Total weight losses of 21.7% (Figure 3a), 30.8% (Figure 3b), 36.5% (Figure 3c), 45.5% (Figure 3d), and 50.6% (Figure 3e), respectively, in the range of 40−850 °C were observed. As a result, nearly 10−15 wt % of the MWCNTs-poly(PEGMMA) composites was composed of thermo-responsive poly(PEGMMA).

We used Raman spectroscopy to evaluate the structural changes in the crystallinity and defect of of CNTs throughout the synthetic process. Figure 4 shows the Raman spectra of pristine MWCNTs, MWCNTs-COOH, MWCNTs-poly(PEGMMA-475), and MWCNTs-poly(PEGMMA-950). All the samples present two bands at 1355 cm^{-1} (D band in disorder-induced mode, which can be attributed to defects) and 1577 cm^{-1} (G band in tangential mode, indicating the

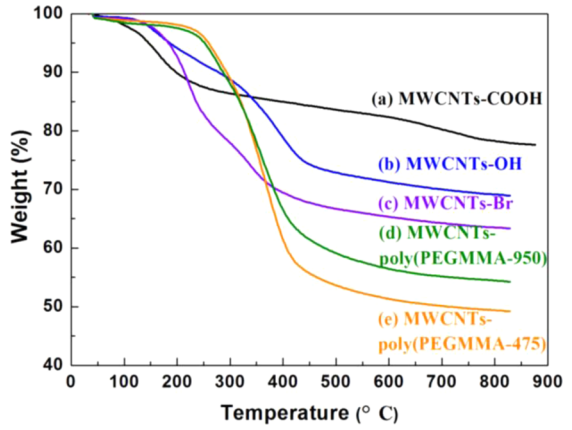

Figure 3. TGA curves of (a) MWCNTs-COOH, (b) MWCNTs-OH, (c) MWCNTs-Br, (d) MWCNTs-poly(PEGMMA-950), and (e) MWCNTs-poly(PEGMMA-475).

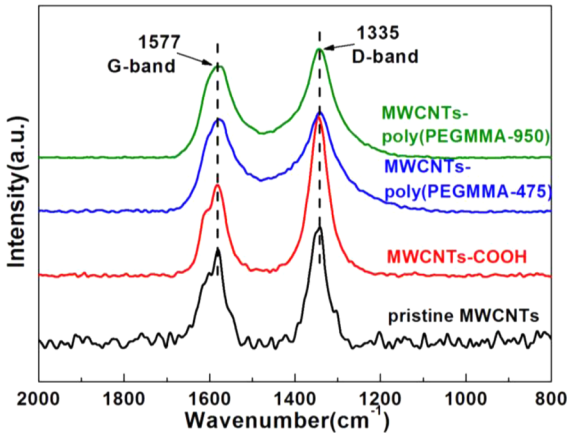

Figure 4. Raman spectra of pristine MWCNTs, MWCNTs-COOH, MWCNTs-poly(PEGMMA-475), and MWCNTs-poly(PEGMMA-950).

formation of well-graphitized CNTs). Compared to that of pristine MWCNTs, only a slight increase in the D band intensity of MWCNTs-COOH was observed, which is due to the fact that only the outer surface of MWCNTs was damaged during treatment with a concentrated acid. However, for MWCNTs-poly(PEGMMA-475) and MWCNTs-poly(PEGMMA-950), only the width of the D band became broadened, leaving the G band nearly unchanged. As a result, even if this broadening in the D band indicates an increase in the level of disorder,[24] the character or property of CNTs was not changed considerably.[25]

3.2. Room-Temperature Surface Wettability and Thermo-Induced Phase Transfer Behaviors of MWCNTs-Poly(PEGMMA). To determine the room-temperature wettability of the polymer-modified MWCNT surface, WCAs toward MWCNTs-COOH, MWCNTs-poly(PEGMMA-475), and MWCNTs-poly(PEGMMA-950) were measured. It can be seen from Figure 5a that the WCAs of MWCNTs-poly(PEGMMA-475) (~45°) and MWCNTs-poly(PEGMMA-950) (~45°) are both smaller than that of MWCNTs-COOH (~60°), because ethylene oxide groups grafted onto MWCNTs make the surface more hydrophilic. This argument can be further confirmed when water droplets are placed on different sample surfaces to record the corresponding infiltration time. It can be stated from Figure

dx.doi.org/10.1021/am405796c | ACS Appl. Mater. Interfaces 2014, 6, 4143−4148

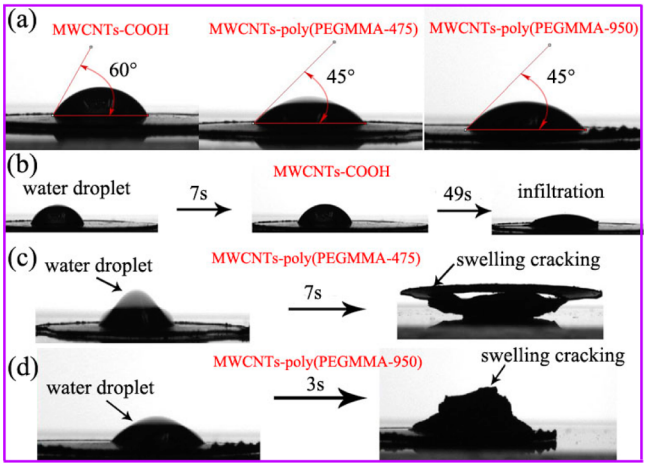

Figure 5. (a) WCAs of MWCNTs-COOH, MWCNTs-poly(PEGMMA-475), and MWCNTs-poly(PEGMMA-950). (b) Infiltration time of water droplets on the MWCNTs-COOH substrate. (c) Infiltration time of water droplets on the MWCNTs-poly(PEGMMA-475) substrate. (d) Infiltration time of water droplets on the MWCNTs-poly(PEGMMA-950) substrate. Sample powders were pressed into pellets before each measurement of WCAs.

5b that the water droplet on the MWCNTs-COOH surface stayed for 49 s before leaking into the substrate beneath, a time much longer than the time it took for the MWCNTs-poly(PEGMMA-475) powder-pressed pellet, 7 s (Figure 5c), and for the MWCNTs-poly(PEGMMA-950) base, 3 s (Figure 5d).

The phase transfer behaviors of MWCNTs-COOH, MWCNTs-poly(PEGMMA-475), and MWCNTs-poly-(PEGMMA-950) between water and [Emim]NTf_2 in response to changes in temperature were studied. Certain amounts of samples were dispersed in deionized water at ambient temperature by ultrasonication, and then an equivalent volume of [Emim]NTf_2 was added to construct a water−ionic liquid biphasic system. From Figure 6a, one can see that over the temperature range of 20−90 °C, MWCNTs-COOH always remains in the [Emim]NTf_2 phase without moving forward to the water phase. This agrees well with the WCA measurements mentioned above, because MWCNTs-COOH is less hydrophilic. In Figure 6b, however, MWCNTs-poly(PEGMMA-475) could only stay in water within the temperature range of 20−40 °C, while at 50 °C, a few samples began to cross the interface and moved into the [Emim]NTf_2 phase instead. All the MWCNTs-poly(PEGMMA-475) samples moved into the [Emim]NTf_2 phase at ∼55 °C and stayed there throughout the temperature range of 60−90 °C. After the samples had been cooled naturally to 20 °C, it was interesting to find that MWCNTs-poly(PEGMMA-475) returned to deionized water spontaneously. The whole process is reversible and repeatable. These results suggest that the reversible water−hydrophobic ionic liquid biphasic transfer in response to temperature variation is endowed by the surface-modified thermo-responsive poly(PEGMMA-475). In Figure 6c, in a similar way, MWCNTs-poly(PEGMMA-950) stay in deionized water at 20−50 °C, while a few samples showed the tendency to move across the interface at 60 °C. All the MWCNTs-poly(PEGMMA-950) were shifted into the [Emim]NTf_2 phase above 80 °C and could also go back to the water phase when the temperature decreased to 20 °C. It is worth noting that the critical phase transfer temperature of MWCNTs-poly-

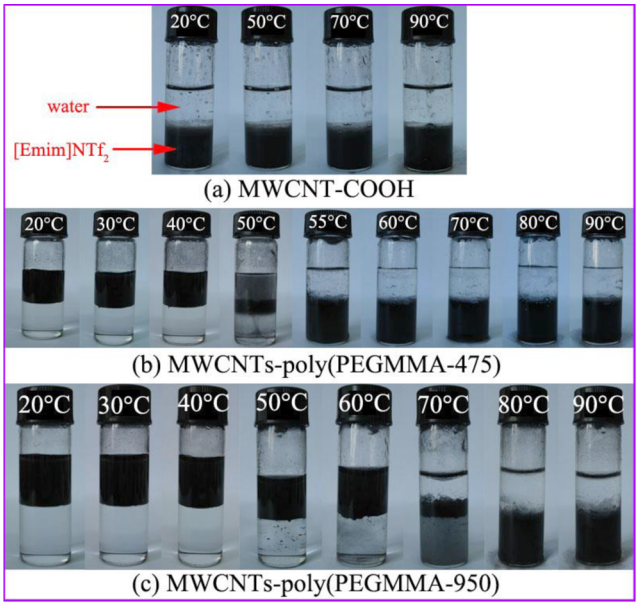

Figure 6. Phase transfer behaviors of (a) MWCNTs-COOH, (b) MWCNTs-poly(PEGMMA-475), and (c) MWCNTs-poly-(PEGMMA-950) between water and [Emim]NTf_2 in response to changes in temperature.

(PEGMMA-950) is higher than that of MWCNTs-poly-(PEGMMA-475) because the side chain of PEGMMA-950 is longer than that of PEGMMA-475, thus demanding a higher driving energy to activate the hydrophilic−hydrophobic transformation of thermo-sensitive segments.

3.3. Interpretation of the Mechanism for the Thermo-Induced Phase Transfer Behavior of MWCNTs-Poly-(PEGMMA). To study the mechanism of the phase transfer behavior of polymer-modified MWCNTs, temperature-dependent ^{1}H NMR spectra were recorded in D_2O, using the methyl signal of sodium 2,2-dimethyl-2-silapentane-5-sulfonate as $\delta = 0$ ppm. From Figure 7, it can be seen that the chemical shifts of protons for poly(ethylene oxide) side chains that were grafted onto MWCNTs gradually decreased with an increase in temperature, confirming the weakened hydrogen bond interactions between poly(ethylene oxide) and water at higher temperatures.[26]

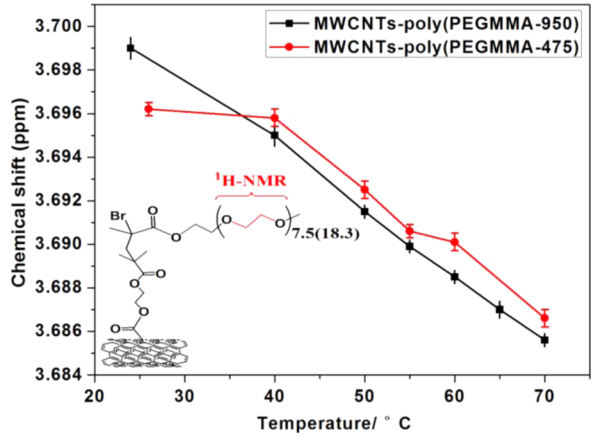

Figure 7. Temperature-dependent ^{1}H NMR measurement for detecting the interactions between poly(ethylene oxide) side chains and water.

dx.doi.org/10.1021/am405796c | ACS Appl. Mater. Interfaces 2014, 6, 4143−4148

On the basis of the results described above and a literature review, a phase transfer mechanism of MWCNTs-poly(PEGMMA) can be proposed as illustrated in Scheme 2.

Scheme 2. Proposed Mechanism for the Temperature Responsive Phase Transfer Behavior of MWCNTs-Poly(PEGMMA)

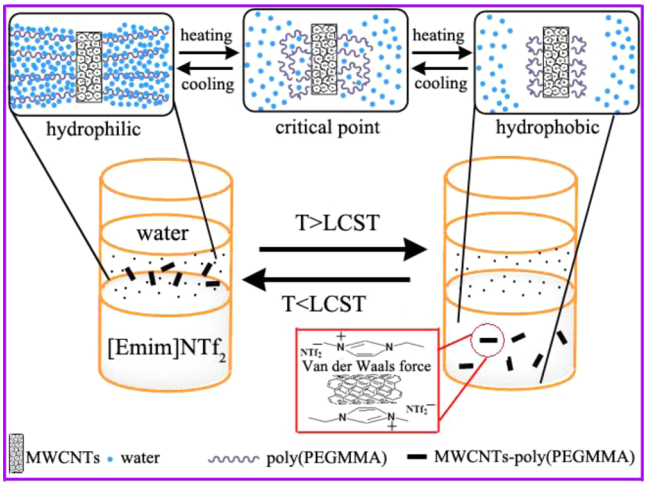

MWCNT-poly(PEGMMA) samples are well dispersed in water because grafted poly(ethylene oxide) side chains generate many hydrogen bonds with water at lower temperatures.[27] However, as the temperature increases, polymers gradually become dehydrated and insoluble; in other words, water becomes a worse solvent for poly(ethylene oxide) groups. At the same time, 1-alkyl-3-methylimidazolium types of ionic liquids are also good solvents for poly(ethylene oxide).[1,28] The difference is that the solvent character of $[Emim]NTf_2$ for poly(ethylene oxide) groups does not change remarkably with temperature as the interaction between $[Emim]NTf_2$ and poly(ethylene oxide) is essentially electrostatic attraction. Of course, we do not exclude the possible $\pi-\pi$ interactions between the 1-ethyl-3-methylimidazole ring and MWCNTs.[8,29] Therefore, the relative affinity of $[Emim]NTf_2$ and water for the poly(ethylene oxide) groups changes with temperature. After reaching a specific point, namely the lower critical solution temperature (LCST),[30] the polymer chains become relatively hydrophobic and prefer to take a self-coiling configuration.[31] As a result, MWCNT-poly(PEGMMA) samples move into the hydrophobic ionic liquid phase.

4. CONCLUSION

In conclusion, thermo-sensitive poly(PEGMMA)-grafted MWCNTs were prepared via surface-initiated ATRP and carefully characterized by TEM, FTIR, TGA, Raman spectra, WCAs, and ^1H NMR measurements. Two representative samples, MWCNTs-poly(PEGMMA-475) and MWCNTs-poly(PEGMMA-950), could both reversibly transfer between water (decreasing the temperature to 20 °C) and hydrophobic ionic liquid $[Emim]NTf_2$ (increasing the temperature to 90 °C) in response to a change in temperature. The reversible phase transfer between water and $[Emim]NTf_2$ is due to the relative affinity of the two solvents for the poly(ethylene oxide) units. These MWCNTs-poly(PEGMMA) may further load nanoparticles (Au, Pt, Pd, etc.) or other substances to serve as phase transfer vehicles as well as heterogeneous catalysts. The related research is underway.

AUTHOR INFORMATION

Corresponding Author

*E-mail: jsguo@dhu.edu.cn. Phone: (+86) 21-6779-2630. Fax: (+86) 411-8437-9992.

Author Contributions

Y.W. and W.L. contributed equally to this work.

Notes

The authors declare no competing financial interest.

ACKNOWLEDGMENTS

This work was supported by the National Natural Science Foundation of China (21273235 and 20173189) and the Knowledge Innovation Program of the Chinese Academy of Sciences.

REFERENCES

(1) He, Y.; Lodge, T. P. Thermoreversible, Intact Transfer of Block Copolymer Micelles between an Ionic Liquid and Water. *J. Am. Chem. Soc.* **2006**, *128*, 12666−12667.

(2) Chechik, V.; Zhao, M.; Crooks, R. M. Self-Assembled Inverted Micelles Prepared from a Dendrimer Template: Phase Transfer of Encapsulated Guests. *J. Am. Chem. Soc.* **1999**, *121*, 4910−4911.

(3) Wu, Y.; Zhang, C.; Qu, X.; Liu, Z.; Yang, Z. Light-Triggered Reversible Phase Transfer of Composite Colloids. *Langmuir* **2010**, *26*, 9442−9448.

(4) Edwards, E. W.; Chanana, M.; Wang, D.; Möhwald, H. Stimuli-Responsive Reversible Transport of Nanoparticles across Water/Oil Interfaces. *Angew. Chem., Int. Ed.* **2008**, *47*, 320−323.

(5) Cole-Hamilton, D. J. Homogeneous Catalysis: New Approaches to Catalyst Separation, Recovery, and Recycling. *Science* **2003**, *299*, 1702−1706.

(6) Desset, S. L.; Cole-Hamilton, D. J. Carbon Dioxide Induced Phase Switching for Homogeneous-Catalyst Recycling. *Angew. Chem., Int. Ed.* **2009**, *48*, 1472−1474.

(7) Horton, J. M.; Bai, Z.; Jiang, X.; Li, D.; Lodge, T. P.; Zhao, B. Spontaneous Phase Transfer of Thermosensitive Hairy Particles between Water and an Ionic Liquid. *Langmuir* **2011**, *27*, 2019−2027.

(8) Wu, B.; Hu, D.; Kuang, Y.; Liu, B.; Zhang, X.; Chen, J. Functionalization of Carbon Nanotubes by an Ionic-Liquid Polymer: Dispersion of Pt and PtRu Nanoparticles on Carbon Nanotubes and Their Electrocatalytic Oxidation of Methanol. *Angew. Chem., Int. Ed.* **2009**, *48*, 4751−4754.

(9) John, J.; Gravel, E.; Hagege, A.; Li, H.; Gacoin, T.; Doris, E. Catalytic Oxidation of Silanes by Carbon Nanotube-Gold Nanohybrids. *Angew. Chem., Int. Ed.* **2011**, *50*, 7533−7536.

(10) Pan, X.; Bao, X. The Effects of Confinement inside Carbon Nanotubes on Catalysis. *Acc. Chem. Res.* **2011**, *44*, 553−562.

(11) Treacy, M.; Ebbesen, T.; Gibson, J. Exceptionally High Young's Modulus Observed for Individual Carbon Nanotubes. *Nature* **1996**, *381*, 678−680.

(12) Coleman, J.; Khan, U.; Gun'ko, Y. Mechanical Reinforcement of Polymers using Carbon Nanotubes. *Adv. Mater.* **2006**, *18*, 689−706.

(13) Qin, S.; Qin, D.; Ford, W. T.; Resasco, D. E.; Herrera, J. E. Functionalization of Single-Walled Carbon Nanotubes with Polystyrene via Grafting to and Grafting from Methods. *Macromolecules* **2004**, *37*, 752−757.

(14) Kong, H.; Gao, C.; Yan, D. Functionalization of Multiwalled Carbon Nanotubes by Atom Transfer Radical Polymerization and Defunctionalization of the Products. *Macromolecules* **2004**, *37*, 4022−4030.

(15) Marcilla, R.; Curri, M. L.; Cozzoli, P. D.; Martínez, M. T.; Loinaz, I.; Grande, H.; Pomposo, J. A.; Mecerreyes, D. Nano-Objects

on a Round Trip from Water to Organics in a Polymeric Ionic Liquid Vehicle. *Small* **2006**, *2*, 507−512.
(16) Huddleston, J. G.; Visser, A. E.; Reichert, W. M.; Willauer, H. D.; Broker, G. A.; Rogers, R. D. Characterization and Comparison of Hydrophilic and Hydrophobic Room Temperature Ionic Liquids Incorporating the Imidazolium Cation. *Green Chem.* **2001**, *3*, 156−164.
(17) Hallett, J. P.; Welton, T. Room-Temperature Ionic Liquids: Solvents for Synthesis and Catalysis. 2. *Chem. Rev.* **2011**, *111*, 3508−3576.
(18) Li, D.; Dunlap, J. R.; Zhao, B. Thermosensitive Water-Dispersible Hairy Particle-Supported Pd Nanoparticles for Catalysis of Hydrogenation in an Aqueous/Organic Biphasic System. *Langmuir* **2008**, *24*, 5911−5918.
(19) Kong, H.; Gao, C.; Yan, D. Controlled Functionalization of Multiwalled Carbon Nanotubes by in situ Atom Transfer Radical Polymerization. *J. Am. Chem. Soc.* **2004**, *126*, 412−413.
(20) Yu, B.; Zhou, F.; Liu, G.; Liang, Y.; Huck, W. T. S.; Liu, W. The Electrolyte Switchable Solubility of Multi-Walled Carbon Nanotube/Ionic Liquid (MWCNT/IL) Hybrids. *Chem. Commun.* **2006**, 2356−2358.
(21) Castillejos, E.; Debouttière, P.; Roiban, L.; Solhy, A.; Martinez, V.; Kihn, Y.; Ersen, O.; Philippot, K.; Chaudret, B.; Serp, P. An Efficient Strategy to Drive Nanoparticles into Carbon Nanotubes and the Remarkable Effect of Confinement on Their Catalytic Performance. *Angew. Chem., Int. Ed.* **2009**, *48*, 2529−2533.
(22) Nasef, M.; Saidi, H.; Dessouki, A.; EI-Nesr, E. Radiation-Induced Grafting of Styrene onto Poly(tetrafluoroethylene) (PTFE) films. I. Effect of grafting conditions and properties of the grafted films. *Polym. Int.* **2000**, *49*, 399−406.
(23) Pielichowska, K.; Gkowinkowski, S.; Lekki, J.; Binias, D.; Pielichowski, K.; Jenczyk, J. PEO/Fatty Acid Blends for Thermal Energy Storage Materials. Structural/Morphological Features and Hydrogen Interactions. *Eur. Polym. J.* **2008**, *44*, 3344−3360.
(24) Casiraghi, C.; Ferrari, A. C.; Robertson, J. Raman Spectroscopy of Hydrogenated Amorphous Carbons. *Phys. Rev. B* **2005**, *72*, 0854011−08540114.
(25) Castelaín, M.; Martínez, G.; Marco, C.; Ellis, G.; Salavagione, H. J. Effect of Click-Chemistry Approaches for Graphene Modification on the Electrical, Thermal, and Mechanical Properties of Polyethylene/Graphene Nanocomposites. *Macromolecules* **2013**, *46*, 8980−8987.
(26) Li, D.; Jones, G. L.; Dunlap, J. R.; Hua, F.; Zhao, B. Thermosensitive Hairy Hybrid Nanoparticles Synthesized by Surface-Initiated Atom Transfer Radical Polymerization. *Langmuir* **2006**, *22*, 3344−3351.
(27) Dormidontova, E. E. Influence of End Groups on Phase Behavior and Properties of PEO in Aqueous Solutions. *Macromolecules* **2004**, *37*, 7747−7761.
(28) He, Y.; Li, Z.; Simone, P.; Lodge, T. P. Self-Assembly of Block Copolymer Micelles in an Ionic Liquid. *J. Am. Chem. Soc.* **2006**, *128*, 2745−2750.
(29) Kim, T. Y.; Lee, H. W.; Kim, J. E.; Suh, K. S. Synthesis of Phase Transferable Graphene Sheets Using Ionic Liquid Polymers. *ACS Nano* **2010**, *4*, 1612−1618.
(30) Bai, Z.; He, Y.; Lodge, T. P. Block Copolymer Micelle Shuttles with Tunable Transfer Temperatures between Ionic Liquids and Aqueous Solutions. *Langmuir* **2008**, *24*, 5284−5290.
(31) Zhang, Y.; Luo, S.; Liu, S. Fabrication of Hybrid Nanoparticles with Thermoresponsive Coronas via a Self-Assembling Approach. *Macromolecules* **2005**, *38*, 9813−9820.